



## Analysis of fault ride through the improvement of PV power plant based on artificial neural network

### Yapay sinir ağına dayalı bir FV güç santralının arızalarının iyileştirilmesi yoluyla analizi

Altan Gencer<sup>1,\*</sup> 

<sup>1</sup> Nevşehir Hacı Bektaş Veli University, Electrical and Electronics Engineering Department, 50300, Nevşehir, Turkey

#### Abstract

The increasing adoption of renewable energy sources in industrial areas, driven by the need to both obtain a grid voltage from renewable energy sources and reduce high electricity bills, has led to an increased demand for solutions that can improve the power quality of these systems. A photovoltaic power plant (PVPP) based on a dc-chopper circuit protection system is proposed for the enhancement of the power quality of PVPP. The aim of the presented protection method is to protect the panels in the PVPP from the harmful effects of the high dc-voltage that occurs during grid faults. The adaptive neural network control system is applied in both the T-type inverter and the dc-chopper circuit protection system. The proposed protection system is implemented with a 250 kW PVPP to verify its validity with simulation results during grid fault. This approach can potentially improve the reliability and stability of PVPP, and contribute to the maintain of PVPP into the grid.

**Keywords:** Photovoltaic power plant, Artificial neural network, dc-chopper circuit,

#### 1 Introduction

The use of solar photovoltaic energy as a source of renewable energy has been gaining significant importance in recent years [1,2]. As a result, the operation and design of photovoltaic power plant (PVPP) have become a crucial issue in relation to electrical grids [3]. The reliability and stability of the power system are crucial in ensuring a safe and efficient power supply and meeting the increasing demand for renewable energy sources [4,5]. Grid faults can occur due to various reasons such as lightning strikes, short circuits, or the connection of large loads on the electrical power grid system [6]. These faults can cause the voltage value in the electrical grid system to fall below its nominal value and can have detrimental effects on devices that are sensitive to voltage fluctuations [7]. It can also lead to a loss of power generation and cause damage to the PVPP system [8]. During a grid fault, the PVPP must be able to stay connected to the grid to prevent power outages. If the voltage value does not recover 90% within 1.5 seconds, the grid-connected PVPP is disconnected from the power system

#### Öz

Hem yenilenebilir enerji kaynaklardan bir şebeke gerilimi elde etme hem de yüksek elektrik faturalarını azaltma ihtiyacından kaynaklanan endüstriyel alanlarda yenilenebilir enerji kaynaklarının giderek daha fazla benimsenmesi bu sistemlerin güç kalitesini iyileştirebilecek çözümlere olan talebin artmasına neden olmaktadır. Fotovoltaik enerji santralının (FVES) güç kalitesinin artırılması için da-kıyıcı devre koruma sistemine dayalı bir fotovoltaik enerji santrali önerilmiştir. Bir da-kıyıcı devre koruma sisteminin temel amacı, FV panelleri şebeke arızaları sırasında oluşan yüksek da-voltajın zararlı etkilerinden korumaktır. Uyarlanabilir sinir ağı kontrol sistemi, hem T tipi eviricinin denetim sistemine hem de da-kıyıcı devre koruma sistemine uygulanmıştır. Önerilen koruma sistemi, şebeke arızası sırasında benzetim sonuçlarıyla geçerliliğini doğrulamak için 250 kW'lık bir FVES ile uygulanmıştır. Bu yaklaşım potansiyel olarak FVES' in güvenilirliğini ve istikrarını artırabilir ve FVES' in şebekeye bağlantısında katkıda bulunabilir.

**Anahtar kelimeler:** Fotovoltaik enerji santrali, Yapay sinir ağı, da-kıyıcı devresi

[9,10]. Therefore, the fault ride-through (FRT) mode of PVPP must be activated during grid faults to ensure continuity of power supply. The FRT mode enables the PVPP system to ride through the fault, generate power, and feed it to the grid [11].

Many successful applications in the literature have been proposed to protect PV systems from the effects of overcurrent and voltage that will occur during grid faults. These proposed protection systems are of two types, software and hardware. Software protection systems are more difficult to implement than hardware protection systems due to the fact that require special expertise. Ref [12] and [13] present a dc-chopper circuit protection scheme for the PV system during grid fault conditions. PI controller is used in the control scheme of dc-chopper circuit protection and PV system. However, The PI control system is a conventional control system. Traditional control systems have difficulty solving complex systems such as PV. Ref [14] presents a static synchronous compensator device (STATCOM) for PV and wind systems, named Wind-

\* Sorumlu yazar / Corresponding author, e-posta / e-mail: altangencer@nevsehir.edu.tr (A. Gencer)  
Geliş / Received: 17.02.2023 Kabul / Accepted: 13.03.2023 Yayınlanma / Published: 15.04.2023  
doi: 10.28948/ngumuh.1252244

STATCOM and PV-STATCOM. However, this approach requires cost and additional equipment. STATCOM also requires the installation of a large amount of storage equipment. The hybrid system has difficulty protecting from over-currents and therefore causes mechanical stress. Ref. [15] implemented a dynamic voltage restorer (DVR) to the PV system during voltage sag. Ref. [16] Smart-Transformers (ST) are applied to improve fault ride-through strategies within a microgrid. However, the DVR and ST systems are more expensive than the dc-chopper system. Each of these methods has its own disadvantages and advantages, and selecting the best method for a specific application will depend on factors such as cost, complexity, and performance.

This article aims to suggest using Artificial Neural Networks (ANNs) to enhance Fault Ride-Through abilities in Photovoltaic systems. The specific objectives of this research include:

- 1) To review the current state-of-the-art in PV FRT, including challenges and limitations of existing approaches.
- 2) To present a case study of using ANNs to improve FRT capabilities of a PVPP, including a detailed explanation of the ANN architecture, training process, and performance results.
- 3) Overall, the main goal of this research is to demonstrate the potential of ANNs as a powerful tool for improving the stability and reliability of grid systems.

## 2 PVPP panel system

Solar PV cells convert sunlight into electrical energy. An equivalent electrical circuit of a PV cell depicts in Figure 1. By using this model, researchers can predict the cell's performance under different conditions and optimize the design of the cell to improve its efficiency. This could pave the way for the creation of solar cells that are both more efficient and cost-effective, and play a crucial role in fulfilling the world's growing energy requirements [17,18].

$$I = I_{sc} - I_0 \left[ \exp \left( \frac{V + R_s I}{\frac{N_s K T}{q} a} \right) - 1 \right] - \left( \frac{V + R_s I}{R_{sh}} \right) \quad (1)$$

If  $V_t = \frac{N_s K T}{q}$  is substituted in Equation (1), Equation

(2) is obtained as follows [17,18].

$$I = I_{sc} - I_0 \left[ \exp \left( \frac{V + R_s I}{V_t a} \right) - 1 \right] - \left( \frac{V + R_s I}{R_{sh}} \right) \quad (2)$$

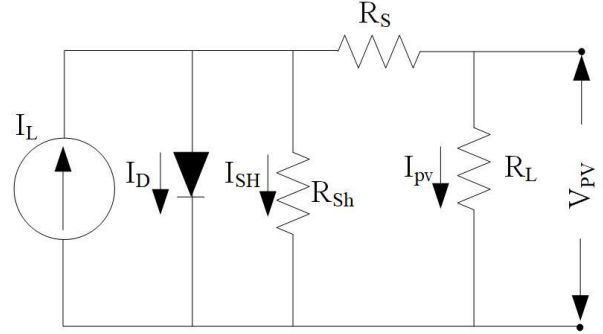


**Figure 1.** The equivalent electrical circuit model of a solar cell [17,18].

$I_{sc}$  depicts a short circuit,  $I_0$  depicts saturation current,  $N_s$  depicts a series connected cell,  $T$  depicts a temperature cell,  $K$  depicts a Boltzman constant,  $R_s$  depicts series resistance,  $R_{sh}$  depicts shunt resistance, and  $q$  depicts the charge of an electron ( $q=1.6 \times 10^{-19} C$ ) [17, 18].

Figure 2 illustrates the T-type inverter, which utilizes fewer semiconductor switches compared to other inverter types, such as the three-level Neutral Point Clamped (NPC) inverter. This reduction in switches results in lower conduction loss and improved efficiency. A T-type inverter method also has a lower harmonic distortion compared to other inverter topologies, which leads to better power quality. The grid-connected PVPP is the most widely used PV system. A general structure of grid-connected PVPP is illustrated in Figure 2. The PV panels of the grid-connected PVPP consist of 7 series connected modules per string and 88 parallel strings. The power of the grid-connected PVPP is 250 kW.

A dc/ac inverter converts a dc voltage obtained from the PV panel output into ac voltage. This inverter generates the ac voltage required to connect the PV panel to a power grid. A T-type inverter requires fewer semiconductor switches than a three-level NPC to obtain the same voltage levels while still performing just as well. Therefore, a T-type inverter is used as dc/ac inverter in this study. Figure 2 shows the T-type inverter, and Table 1 lists its different switching states. Auxiliary switches are used in T-type inverters. The auxiliary switch is used to clamp the dc-link midpoint and a leg of each phase reduces the number of semiconductor switches. A negative level "N" employs a similar number of switches to a positive cycle. Therefore, T-type topology has higher efficiency and lower conduction loss than three-level NPC [19].

Each phase output of a 3-phase system is obtained by using semiconductor switches namely Q1, Q2, Q3 and Q4. These switches are on or off for the positive or negative periods of the sinusoidal wave. When Q1 is on, the current flows from  $V_{dc}$  (+) to the output and the output voltage is positive. When Q1 is off, current flows through Q3/D2. The simple delay time is applied during the on-off time. A short circuit in the dc-link is prevented using this delay time. This delay time is set to 1 ms. When Q2 is on, the current flows from  $V_{dc}$  (-) to the output and negative output voltage. When Q2 is off, current flows through Q3/D2 [19].

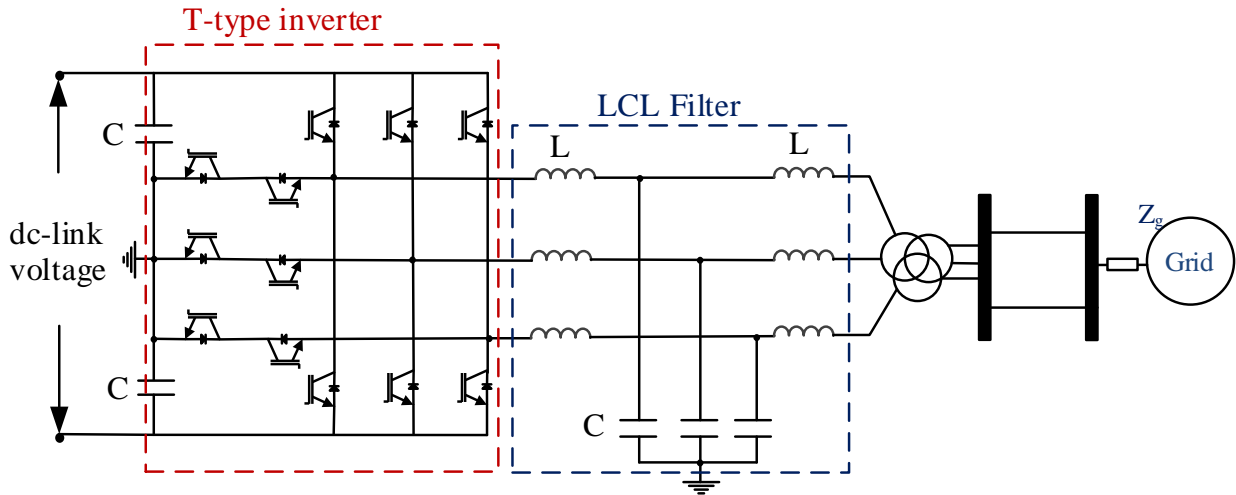


Figure 2. The T-type inverter for the grid-connected PVPP.

Table 1. Voltage Levels and Switching States in a T-type inverter [19].

Level	Q <sub>1</sub>	Q <sub>2</sub>	Q <sub>3</sub>	Q <sub>4</sub>	Phase voltage
P	0	0	1	0	$V_{dc}/2$
0	0	1	0	1	0
N	1	0	0	0	$-V_{dc}/2$

A T-type inverter has the same switching structure as a three-level NPC. However, the three-level NPC has two extra switching devices, which complicates the control of its system.

### 3 Short circuit analysis of the grid-connected PVPP system

High-level currents occur in power systems during grid faults. Protection systems are designed to protect against the harmful effects of these high currents. The protection system protects the power system from the harmful effects of high-level currents during grid faults. If these protection systems are not well designed, high-level currents can cause serious damage to the power system.

A dc-chopper circuit system consisting of a self-turn-off device IGBT, and a resistor is given in Figure 3. Many protection methods are used in the literature. The dc-chopper circuit system is widely used with its lowest cost and simple structure among these methods. A dc-chopper circuit system is placed between the PV panels and the ac inverter. A switch signal of the IGBT in the protection system is off in normal operation. Therefore, a dc-chopper circuit is disabled during normal operation. A dc-chopper circuit does not affect the PV operation and supplies the grid system during normal operation. A dc-chopper circuit system works by detecting overvoltage in dc-link voltage. When value of dc-link voltage rises, a protection control system sends on-and-off signals to the IGBT. Therefore, the PV panel system will be protected from the harmful effects of over-voltages that will

occur during grid faults. When a dc-link voltage returns to a normal level, a dc-chopper circuit system will be disabled. The PV is quickly restarted and supplies the grid system. The current capacity of the IGBT in the dc-chopper circuit is chosen higher due to the fact that a high current will pass through the protection circuit [12,13,20].

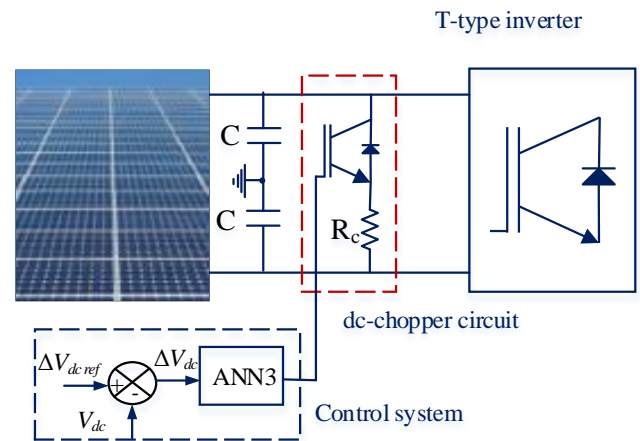


Figure 3. A dc-chopper circuit [12,13,20].

### 4 Proposed control system for PVPP

A proposed control system for PVPP is given in Figure 4. This study applies the grid-connected PVPP to realize the proposed T-type inverter power control optimization and conversion. The control system for the T-type inverter includes all the essential control methods necessary for the PVPP system to connect to the grid. A control system of an inverter is the most important part of a grid-connected PVPP. In Figure 4, the inverter control diagram is illustrated for normal operation. A control diagram of a grid-connected PVPP consists of two loops. The first loop is an  $i_d$  current, which controls the amplitude of the  $V_{dc}$  voltage. The T-type inverter's input dc-link voltage must have a value in the nominal operating range.

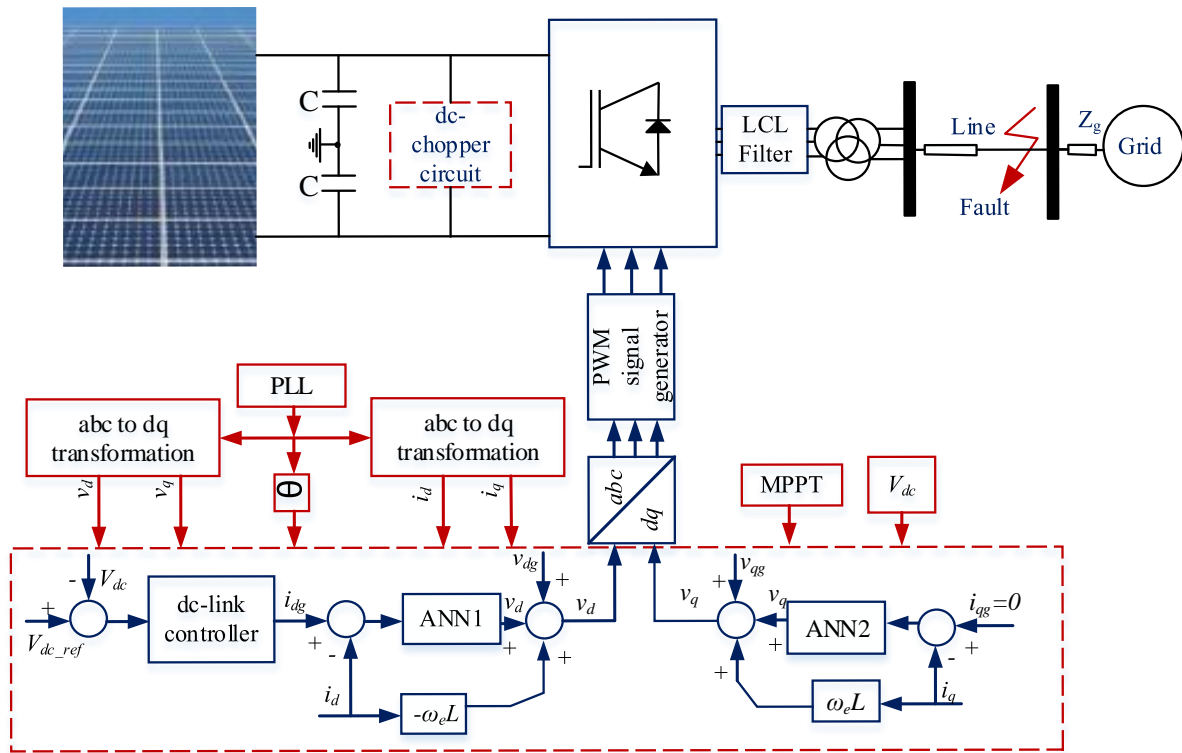


Figure 4. Proposed control system for PVPP

Therefore, a dc-link voltage is chosen as 481 V. A second cycle is the  $i_q$  current.  $i_q$  current value is selected as 0. ANN1 is designed to regulate the  $i_d$  current and ANN2 is designed to regulate the  $i_q$  current. The Levenberg Marquardt algorithm is used to train ANN1 and ANN2 datasets. In order to create the feedforward network, 10 neurons are selected for the hidden layer. ANN1 and ANN2 are generated using 2500 datasets of chosen  $i_d$  and  $i_q$  current values. The datasets are randomly divided with 15% being used for testing, another 15% for validation, and the remaining 70% for training purposes.

## 5 Simulation results

The block diagram of the grid-connected PVPP is designed for 250 kW. A simulation of grid-connected PVPP is realized using Matlab/Simulation. An asymmetrical fault is three phase-to-ground (3LG) fault. The 3LG fault is implemented between  $t=1s$  and  $t=1.1s$  on the grid system.

The dc-link voltage of a 250 kW PVPP with and without the dc-chopper circuit protection system under a 3LG symmetrical fault is illustrated in Figure 5. In order for a PVPP to maintain connected to a power grid, the PV panel's output voltage ( $V_{dc}$ ) must be kept constant at 480V. The unprotected system oscillates between 500V and 600V of dc-link voltage value after a grid fault. Therefore, a PVPP system cannot be connected to a power grid. The dc-link voltage value of a PVPP system with a dc-chopper circuit reaches 480V after a grid fault. PV panel system mains continue to connect with the grid.

Active power of a 250 kW PVPP with and without the dc-chopper circuit protection system under 3LG symmetrical

fault is depicted in Figure 6. The PV panel's output active power must be kept constant at 250 kW. An active power of PVPP with unprotected method oscillates between 250kW and -500kW when a fault is implemented to the system. An active power of PVPP with a dc-chopper circuit reaches 250 kW again shortly after the fault is applied. At the same time, the PV panel system continues to inject 250 kW of active power into the grid.

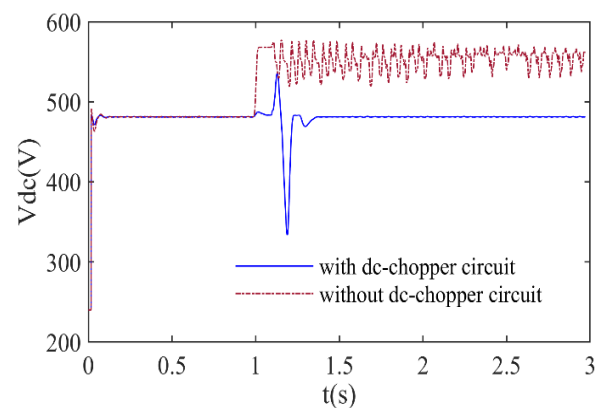


Figure 5. The dc-link voltage of a 250 kW PVPP with and without the dc-chopper circuit protection system under 3LG symmetrical fault

The phase-to-phase output of the T-type inverter without a filter is illustrated in Figure 7. The switching signals of the IGBT of an unprotected system are distorted when the fault



is applied to the system. Therefore, the shape of the sine wave obtained at the output of the inverter is also distorted.

A phase-to-phase output of the T-type inverter without a filter is illustrated in Figure 8. When the fault is applied to the system, the switching signals of the IGBT of a protected system with a dc-chopper circuit are quite smooth. Therefore, a shape of a sine wave obtained at the output of the inverter is also smooth.

The error histogram plot of the ANN1 model is given in Figure 9. The total error of the ANN1 is range from -0.00301 to 0.003655. There is an error rate of 0.000497 in the validation dataset, which consists of 2500 samples in a bin.

The regression values (R) of the test phase, validation, and training of ANN1 are 0.99954, 0.99957, and 0.99952, respectively. These figures are given in Figure 10. This value of R is nearly equal to 1. Therefore, the accuracy value of R is reliable for ANN1 training.

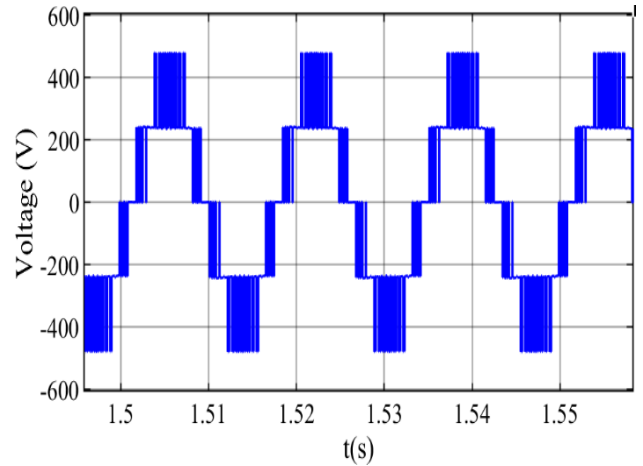


Figure 8. Non-filter of output voltages of the T-type inverter during grid fault with protection system.

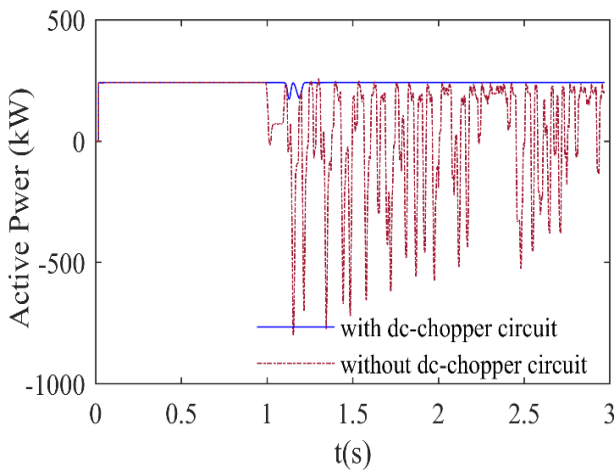


Figure 6. Active power of a 250 kW PVPP with and without the dc-chopper circuit protection system under 3LG symmetrical fault

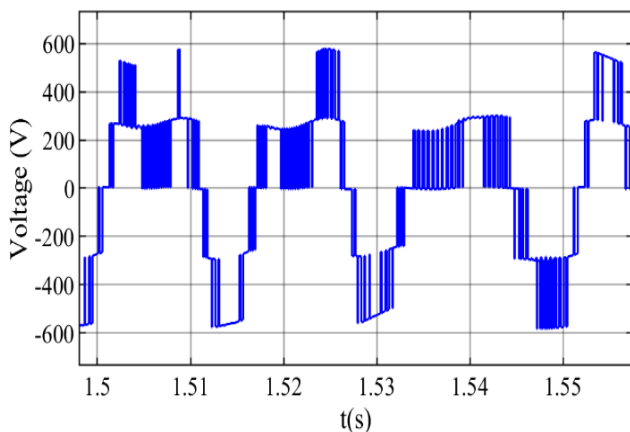


Figure 7. Non-filter of output voltages of the T-type inverter during grid fault with an unprotected system.

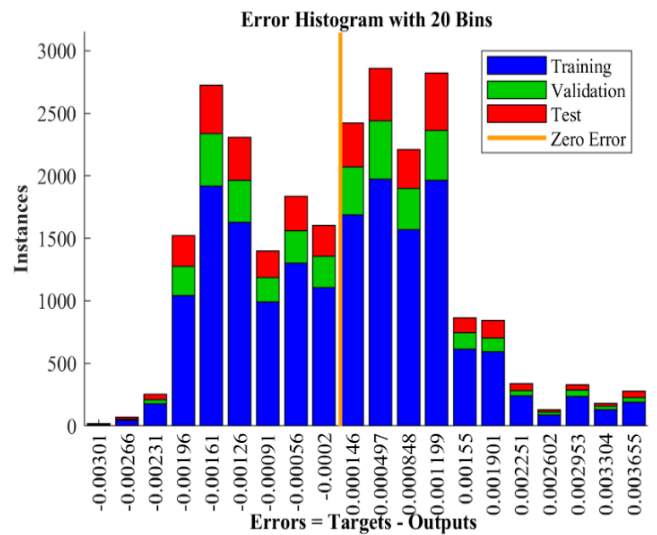


Figure 9. The error histogram plot of ANN1.

## 6 Conclusion

Fault ride through the improvement of PVPP based on the ANN system has the potential to greatly improve the reliability and stability of grid system. The ANN-based approach has several advantages over traditional methods, including its ability to model and predict nonlinear and dynamic systems and its robustness to system uncertainties. The switching signals of the IGBT of presented system with a dc-chopper circuit are quite smooth while the switching signals of IGBT of an unprotected system are distorted during grid fault. The active power of PVPP with a dc-chopper circuit reaches 250 kW again shortly after grid fault while an active power of PVPP with unprotected system oscillates between 250kW and -500kW even after the grid fault. This study presented also demonstrated the effectiveness of using ANN for FRT improvement in PV systems.

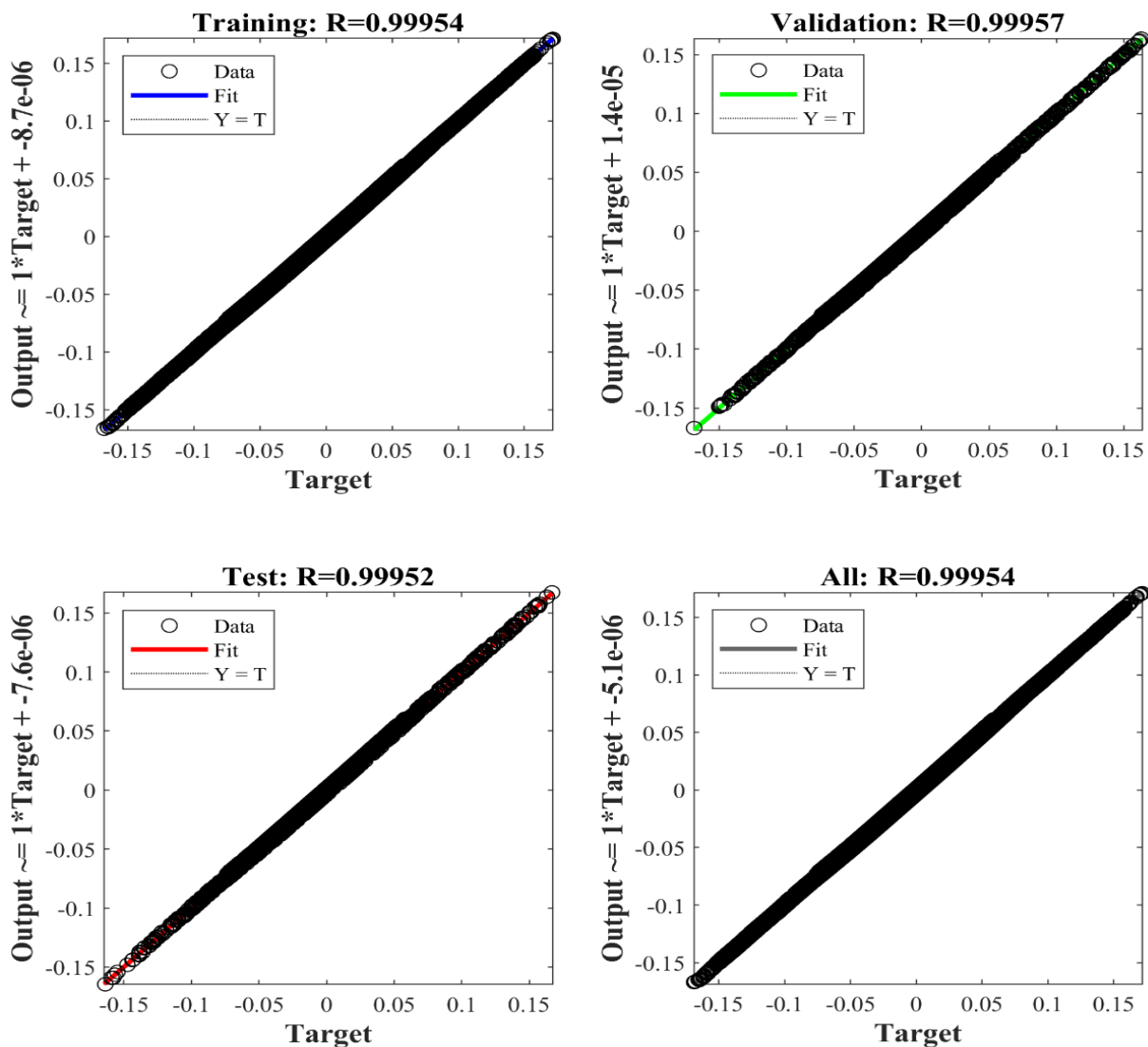


Figure 10. Regression plot of ANN1 model.

#### Declaration of Competing Interest

The authors declare that they have no known competing financial interests or personal relationships that could have appeared to influence the work reported in this paper.

Similarity rate (iThenticate): %7

#### References

- [1] I. Isakov and I. Todorovic, Power production strategies for two-stage PV systems during grid faults, *Solar Energy*, 221, 30-45, 2021 <https://doi.org/10.1016/j.solener.2021.03.085>.
- [2] C. Wang, C. Mishra and V. A. Centeno, A Scalable Method of Adaptive LVRT Settings Adjustment for Voltage Security Enhancement in Power Systems With High Renewable Penetration, in *IEEE Transactions on Sustainable Energy*, 13(1), 440-451, 2022, <https://doi.org/10.1109/TSTE.2021.3116102>.
- [3] H. Mei, C. Jia, J. Fu and X. Luan, Low voltage ride through control strategy for MMC photovoltaic system based on model predictive control, *International Journal of Electrical Power & Energy Systems*, 125, 106530, 2021, <https://doi.org/10.1016/j.ijepes.2020.106530>.
- [4] M. Talha, S.R.S. Raihan and N A. Rahim, PV inverter with decoupled active and reactive power control to mitigate grid faults, *Renewable Energy*, 162, 877-892, 2020, <https://doi.org/10.1016/j.renene.2020.08.067>.
- [5] I. R. S. Priyamvada and S. Das, Adaptive Tuning of PV Generator Control to Improve Stability Constrained Power Transfer Capability Limit, in *IEEE Transactions on Power Systems*, 37 (3), 1770-1781, 2022, <https://doi.org/10.1109/TPWRS.2021.3114704>
- [6] H. M. Hasanien, An Adaptive Control Strategy for Low Voltage Ride Through Capability Enhancement of Grid-Connected Photovoltaic Power Plants, in *IEEE Transactions on Power Systems*, 31(4), 3230-3237, 2016. <https://doi.org/10.1109/TPWRS.2015.2466618>.
- [7] J. P. Roselyn, C. P. Chandran, C. Nithya, D. Devaraj, R. Venkatesan, V. Gopal and S. Madhura, Design and

- implementation of fuzzy logic based modified real-reactive power control of inverter for low voltage ride through enhancement in grid connected solar PV system, *Control Engineering Practice*, 101, 104494, 2020, <https://doi.org/10.1016/j.conengprac.2020.104494>.
- [8] A. Mojallal and S. Lotfifard, Enhancement of Grid Connected PV Arrays Fault Ride Through and Post Fault Recovery Performance, in *IEEE Transactions on Smart Grid*, 10(1), 546-555, 2019, <https://doi.org/10.1109/TSG.2017.2748023>.
- [9] E. Z. Bighash, S. M. Sadeghzadeh, E. Ebrahimzadeh and F. Blaabjerg, Improving performance of LVRT capability in single-phase grid-tied PV inverters by a model-predictive controller, *International Journal of Electrical Power & Energy Systems*, 98, 176-188, 2018, <https://doi.org/10.1016/j.ijepes.2017.11.034>.
- [10] M. J. Morshed and A. Fekih, A Novel Fault Ride Through Scheme for Hybrid Wind/PV Power Generation Systems, in *IEEE Transactions on Sustainable Energy*, 11(4), 2427-2436, 2020, <https://doi.org/10.1109/TSTE.2019.2958918>.
- [11] R. Aljarrah, H. Marzooghi, J. Yu and V. Terzija, Sensitivity analysis of transient short circuit current response to the penetration level of non-synchronous generation, *International Journal of Electrical Power & Energy Systems*, 125, 106556, 2021, <https://doi.org/10.1016/j.ijepes.2020.106556>.
- [12] A. Al-Shetwi, M. Z. Sujod and F. Blaabjerg, Low voltage ride-through capability control for single-stage inverter-based grid-connected photovoltaic power plant, *Solar Energy*, 159, 665-681, 2018, <https://doi.org/10.1016/j.solener.2017.11.027>.
- [13] A. M.A. Haidar and N. Julai, An improved scheme for enhancing the ride-through capability of grid-connected photovoltaic systems towards meeting the recent grid codes requirements, *Energy for Sustainable Development*, 50, 38-49, 2019, <https://doi.org/10.1016/j.esd.2019.02.007>.
- [14] R. Kumar, S. Diwania, R. Singh, H. Ashfaq, P. Khetrapal and S. Singh, An intelligent Hybrid Wind–PV farm as a static compensator for overall stability and control of multimachine power system, *ISA Transactions*, 123, 286-302, 2022, <https://doi.org/10.1016/j.isatra.2021.05.014>.
- [15] S. Kumari, M. D. Mahapatra and S. Pati, Voltage Profile Enhancement in a PV Connected Hybrid Power System using Dynamic Voltage Restorer, 3rd International Conference on Electronics and Sustainable Communication Systems (ICESC), 236-240, India, 17-19 August 2022, <https://doi.org/10.1109/ICESC54411.2022.9885632>.
- [16] J. Rodrigues, C. Moreira and J. P. Lopes, Fault-ride-through strategies for grid-tied and grid-forming smart-transformers suited for islanding and interconnected operation, *Electric Power Systems Research*, 189, 106616, 2020, <https://doi.org/10.1016/j.epr.2020.106616>.
- [17] R. B. Roy et al., A Comparative Performance Analysis of ANN Algorithms for MPPT Energy Harvesting in Solar PV System, in *IEEE Access*, 9, pp. 102137-102152, 2021, <https://doi.org/10.1109/ACCESS.2021.3096864>.
- [18] M. K. Mishu, M. Rokonzaman, J. Pasupuleti, M. Shakeri, K. S. Rahman, S. Binzaid, S. K. Tiong and N. Amin, An adaptive TE-PV hybrid energy harvesting system for self-powered IoT sensor applications, *Sensors*, 21 (8), 2604, 2021, <https://doi.org/10.3390/s21082604>.
- [19] A. Gencer, Comparison of T-Type Converter and NPC for the Wind Turbine Based on Doubly-Fed Induction Generator. *Balkan Journal of Electrical and Computer Engineering*, 9 (2), 123-128, 2021. <https://doi.org/10.17694/bajece.826624>
- [20] A. Gencer, Analysis and Control of Fault Ride Through Capability Improvement PMSG Based on WECS Using Active Crowbar System During Different Fault Conditions. *Elektronika Ir Elektrotehnika*, 24 (2), 63-69, 2018. <https://doi.org/10.5755/j01.eie.24.2.20637>

